MASTER DE CHIMIE PARIS CENTRE
Parcours: Ingénierie Chimique

Rapport de stage 5C101

Small scale Synthesis of Metallic Uranium from Uranium Oxide for Nuclear Forensics applications

MERCIER Alexia

COTE Gérard

University of Nevada, Las Vegas

Index

Introduction

Nuclear Forensics

Radioactive specimens are sensitive materials which need high traceability and accounting as they have a dual use, both in civilian applications such as power plants, as well as in military applications such as nuclear devices.

According to Kenton J. Moody[1] , nuclear forensics objectives are “ to determine the attributes of questioned radioactive specimens.” The scope of the attributes is large. It encompasses caracteristics such as its source, routes and means of transportation, but in the context of this radiochemistry project, it more specifically means defining the synthesis routes and special processes, as well as the signatures the latters leave on the radioactive specimen of interest.

Uranium Chemistry – Metal state, Fuel processing and nuclear device applications

Most nuclear power plants use UO_2 as fuel for conveniance despite it’s lower density of fissile material compared to $U_{(m)}$. For instance, the oxide has a higher melting point than pure uranium metal, doesn’t expand as much under operating conditions, and the oxide can’t spontaneously ignite contrary to the metal form which is poryporphiric especially if finally divided in powder[2]. The study of $U_{(m)}$ is therefore more related to nuclear devices.

One of the main industrial method to produce $U_{(m)}$ was developped by the German chemist Goldschmit at the end of the 19th century, and furthered improved during the Manhattan Project. It is now known as the Ames process. In this process, Uranium Fluoride is mixed with Calcium or Magnesium powder in a sealed crucible commonly called a bomb and then inserted in a furnace, eventually leading to a metal ingot. However, this method can’t be scaled down to gram quantities because the exothermic reaction cannot sustain and cannot produce enough heat to melt the reactants and isolate the uranium metal from the slug.[2]

Considering the need for small uranium metal amounts for specialized chemistry experiments[3], and considering that malicient players would probably not develop industrial infrastructures to produce $U_{(m)}$ for unauthorized nuclear devices, new small scales synthesis routes need to be investigated.

The global approach of this project is to find new small scale synthesis routes for metallic uranium and determine if they leave chemical and/or physical signatures. Two routes will be explored in this project : reduction of Uranium Halides by thermal decomposition with the help of an arc melter, and metallothermic reduction with Dysprosium(II) Iodide. All the reactions and setups will be tested with Cerium Halides first, as Cerium is commonly admitted to be a non-radioactive chemical analogue of Uranium. This study will focus on UI_x and CeI_x compounds.

As isotopes are known to have similar chemical properties, all the experiments will be done with depleted uranium, containing nearly only ^{238}U, which has a longer half-life than ^{235}U and which is fissile with fast neutrons only.

Cerium Chemistry

Every reaction and setup was first tested with Cerium, commonly admitted to be a chemical analogue of Uranium. It shares a lot of similar properties with Uranium except that the naturally occuring Cerium isotopes are all non-radioative. In fact, the common oxidation states of the lanthanides is +III, but Cerium is also found in the +IV state, explained by the stability of the $4f^0$ configuration. It is the only lanthanide able to form the tetrahalide CeF_4 [4]. Furthermore, despite Cerium being 4f and Uranium being 5f, both compounds have very similar ionic radii at the +III and +IV oxidation states. These are our states of interest. According to Shannon[5], the ionic radii of Ce and U are respectively 0.87 vs. 0.89 Å for the +IV state, and 1.01 vs. 1.03 Å for the +III state.

Experimental Methods

Schlenk Line

Two types of borosilicate tubes are used : narrow tubes purchased, with an outside diameter of 10mm and inside diameter of 8mm (thickness 1mm), and wide tubes with an outside diameter of 15.9mm and inner diameter of 12.7mm (thickness 1.6mm). Both are purchased from Chemglass. Starting from 1.5m long glass segments, smaller segments of 30cm are cut and sealed on one end with the methane flame torch.

Sample preparation : Before inserting the reactants, the tube is dried under vacuum on the schlenk line. Once the reactants are at the bottom of the tube, the tube is quickly dried under vacuum a second time to make sure there are no residual oxygen or water. This step should be quick as I_2 has low melting and boiling points and tends to vaporize (which is noticeable by a purple coloration inside the tube). Once the tube is dry and free of oxygen, the bottom of the tube is dipped into liquid nitrogen to make sure all the reactants remain under solid phase during the sealing step. Remnant oxygen should be noticeable as it would condense and form droplets at the bottom. If it is the case, then the tube needs to be heated again, to avoid overpressure in the further steps. Finally, still under vacuum, sealing is achieved by carefully heating the sides of the tube at a length of about 20cm, until the glass collapses on itself.

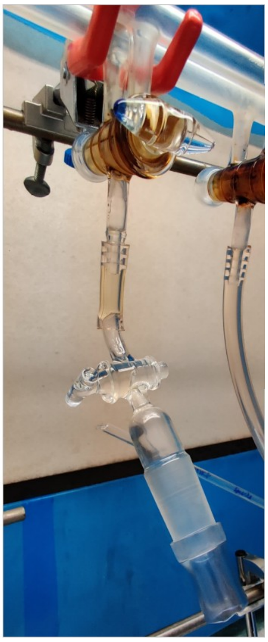

Figure 1: On the left - Schlenk line setup : Vacuum pump (blue), flame torch (red), LN2 container (orange), joint (pink), schlenk line (green).
On the right – joint details : Tygon narrow tube – repurposed round flask cap – Tygon large tube

Furnace

The heating reactions take place in a Thermo Scientific Lindberg Blue M Mini-Mite horizontal tube furnace. The ampoules are put in the middle of the furnace, and glass fiber is placed on both extremities to ensure insulation. Aluminum foil is wraped in a thin smooth layer for the recrystalisation attempts.

Arc Melter

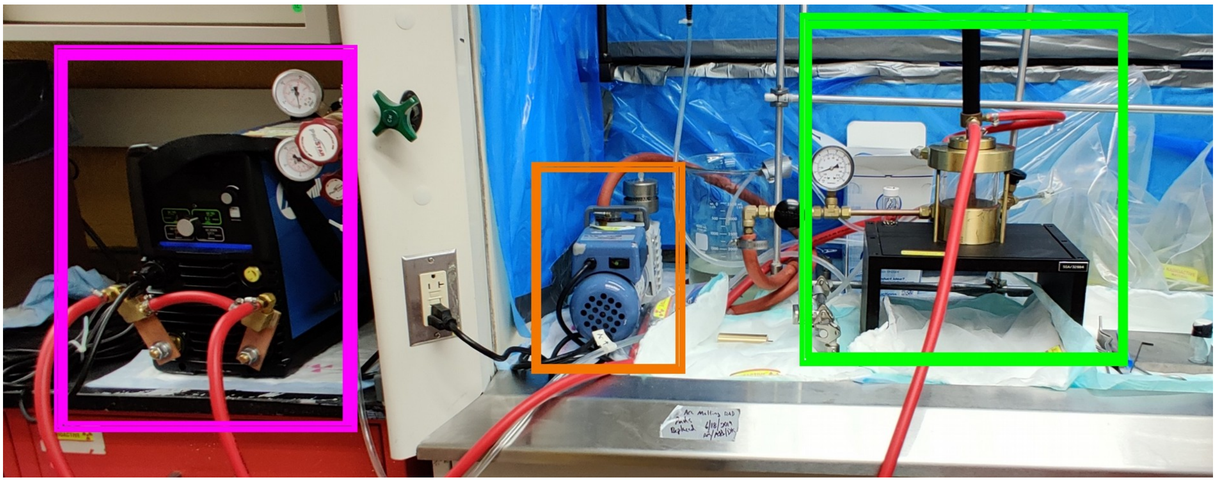

Figure 2: Arc melting setup- Arc melting chamber (green), pump (orange), generator (pink)

The arc melting setup is made of a Miller Maxstar 210 power generator, a Centorr VAC 5SA arc melter, and a vacuum pump. The electrode is made of tungsten. The samples are placed in a costum-drilled copper hearth which is placed on top of the copper crucible.

Figure 3: costum-drilled copper hearth

The sample of interest is placed in a dedicated cavity. The relevant getters are placed in the other cavities or on top of the hearth. The copper hearth is then placed in the arc melting chamber crucible. The chamber is purged three times for three minutes with Argon. Finally the chamber is left at 50 kPa $Ar_{(g)}$ to enable the formation of plasma.

When ready, the generator is turned on, and the electrode is brought to the bottom of the crucible touching the copper. The operator then presses the power pedal while pulling the electrode up. The plasma arc formed is then hovered over the getters and the sample. However the electroce should never directly touch them.

Powder XRD

Powder X-Ray diffraction studies were performed in a Bruker D8 Advance diffractometer equipped with a Cu k-α monochromated x-ray source (λ = 1.5406 Å) and a Lynxeye position sensitive detector with a 3° scan window. Pulverized samples are mounted on a low background silicon stage holder with a thin layer of grease. Diffraction patterns are analyzed using the Bruker Diffrac.Eva software and matched to the database.

SEM

Scanning electron microscope studies were performed in a JEOL JSM-5610, containing a tungsten filament electron gun, equipped with a secondary and backscattered electron detectors and an Oxford ISIS EDS system.

For our studies, the samples were stuck on carbon tape and inserted in the analytical chamber under vacuum. We used an electron beam voltage of 15kV and a working distance of 19mm. Quantification is performed with Inca Software.

Experiments

Cerium(III) Iodide synthesis

Synthesis

Cerium(III) iodide was synthesized based on the experimental procedure of the U(IV) iodide synthesis described by Kraus *et. Al[6]*. We assume that the synthesis reaction goes as follows :

$$3\ CeO_2 + 9/2\ I_2 + 2Al \rightarrow 3\ CeI_3 + 2\ Al_2O_3$$

Two types of batches were tested : small batches and large batches. The first experiments focused on small batch syntheses to make sure the chemistry worked. The syntheses happened in borosilicate ampoules of r_{si} = 0.4cm, L_s = 20cm, V_s = 10cm^{-3}.

To do large batch synthesis a first setup in a 100cm^{-3} round flask was tested. All the reactants in solid state were inserted in the flask, which was then capped and maintained in a heating mantle. However the I_2 gas would remain on top of the flask, recrystallize at the top of the neck, and therefore not react with the other compounds. There were also high risks of the cap popping out and allowing leaks of I_2 gas. Therefore this setup was replaced by an ampoule setup.

Figure 4 : large batch first round-flask setup. I_2 gas is floating above the other reactants, and I_2 can be spoted in the neck of the flask.

Starting from wider and thicker glass segments meant to withstand the I_2 high pressure, ampoules of r_{li} = 12.7mm, L_l = 20cm, V_l = 20cm^{-3} were sealed. Following the same procedure as for the small batch synthesises, the reactants were put in the dried ampoules which were then sealed on the schlenk line under vacuum, and finally put in the tube furnace at different temperature ramps (see Fig 5 and 6).

Several stoichiometries were tested in order to limit excess I_2, keep the partial pressure of I_2 below 1.5 atm, and limit the waste of reactants. Eventually the masses were narrowed down to the following values :

Table 1: Reactant quantities for synthesis of CeI3 depending on the type of batch

	$CeO_{2(s)}$ mg	mmol	**$Al_{(m)}$** mg	mmol	**$I_{2(s)}$** mg	mmol
Small batch, ampoule volume = 10cm^{-3}	14.3	0.083	5.34	0.198	43.6	0.172
Large batch, ampoule volume = 20cm^{-3}	143	0.83	53.4	1.98	436.5	1.72

The two graphs below show the two temperature ramps used.

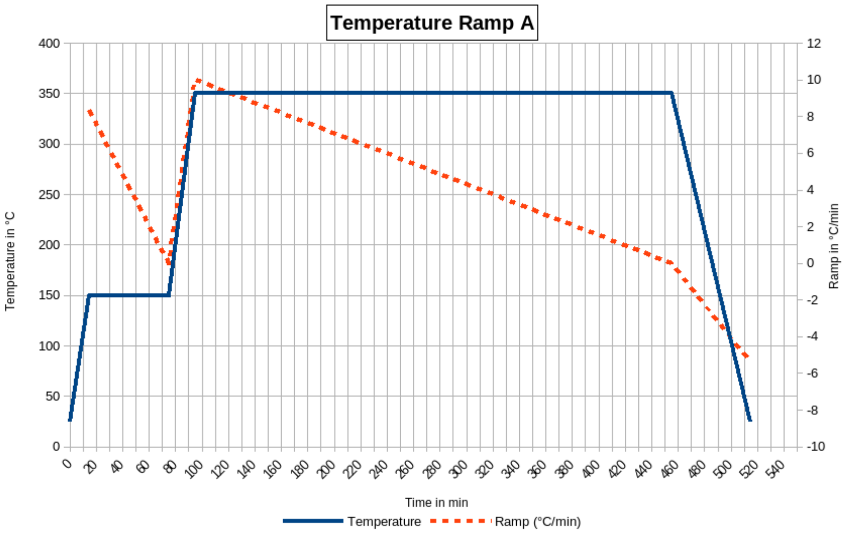

Figure 5: Ramp A 25 - 150 (1h) - 350 (6h)- 25

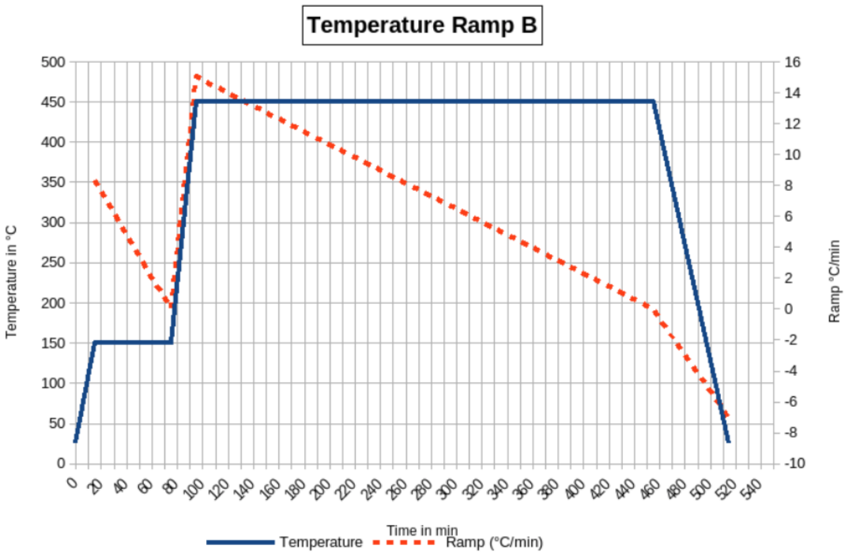

Figure 6: Ramp B 25 – 150 (1h) – 450 (6h) - 25

The temperature ramps led to different behaviours. Ramp A resulted in yellow-lime crystals and white deposits in both small batches and large batches.

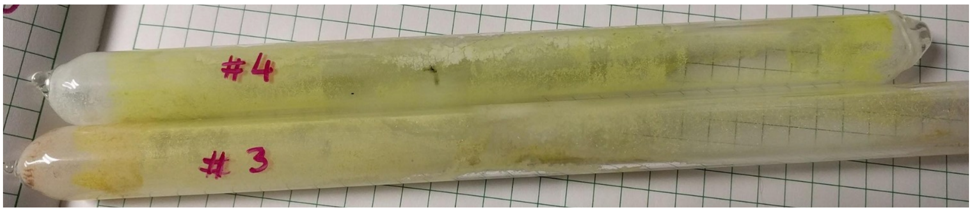

Figure 7: Large batch ampoules after Ramp A. Yellow-lime crystals and white deposits.

However the maximum temperature of Ramp B seemed too high. The glass ampoules all contained a red powder with well-recrystallized I_2 on both extremities.

Figure 8: Large batch ampoule after Ramp B. Air sensitive red powder and recrystallized I2

Even after attempts to put the ampoules back in the tube furnace for another cycle following ramp A, the products didn’t change. The compounds were analyzed by P-XRD. See **Results**.

To confirm that the yellow-lime crystals are a compound of Cerium and Iodide and that the three reactants are needed in this pathway, three sub-experiments were done. For each, two of the three reactants were sealed in small ampoules with small batch quantities, then put in a tube furnace following ramp A.

Table 2: Reactants quantities for CeI3 sub-tests.

	CeO_2 (mg)	**Al** (mg)	**I_2** (mg)	Result
Test #1	15.7		52	No reaction
Test #2		7.7	53	White powder (probably AlI_3) and yellow oily droplets (probably AlI_3•$6H_2O$)
Test #3	15.8	8.3		No reaction

It appears that none of the tubes resulted in yellow lime crystals, which suggests that the three reactants are needed to obtain the CeI_3 and which suggests that the reaction pathway includes an AlI_3 intermerdiary.

Figure 9: Sub-experiments. From left to right : test #1, test #2 and test #3

In situ chemical vapor transportation

In order to better understand the behaviour of each product and try to purify CeI_3 it was decided to reproduce the *in situ* chemical vapor transportation reaction described by [6]. The experiment also allows to verify whether the borosilicate sealed ampoules can withstand the high I_2 pressure before moving on to the radioactive UI_3 compound.

Table 3: Vapor transportation reactant quantities test 1

Compound	CeO_2	Al	I_2
Mass (mg)	172,5	65,5	2673

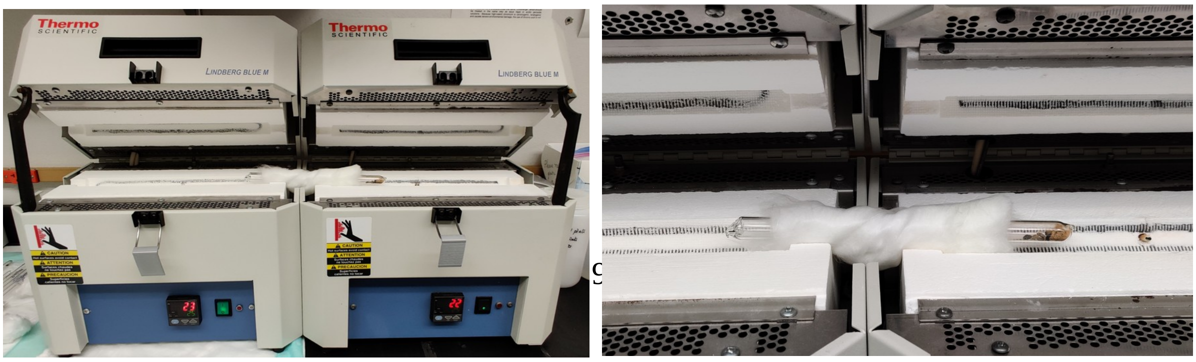

Figure 10: Left - In situ chemical vapor transportation setup. Left furnace is sink, right furnace is source. Right - Close up. The borosilicate ampoule with the reactants concentrated on the right side is placed in both furnaces. The middle section is wrapped in aluminium foil and in glass fiber to ensure heat conduction and prevent heat loss at the junction of the furnaces.

Unfortunately there were no tube furnace with internal temperature gradient available, so two identical tube furnaces were put one next to another and each programmed to their own temperature ramp. The right tube furnace acted as the source, that is the hotter end, and the left tube furnace acted as the sink, that is the colder end. Both furnaces followed the same initial ramp A (see fig. 5): 25°C ↗150°C ↗350°C(6h). The left furnace then stayed at 350°C (sink) while the right furnace temperature increased to 450°C (source). The gradient was maintained for 4 days before the tube was brought back to room temperature.

After 4 days the furnace was opened, but unfortunately it seemed that the ampoule blew out because of I_2 overpressure. It was calculated that the I_2 inner pressure could have reached up to 30 atm.

Figure 11: Burst out ampoule in furnace and inside insulation layer

A second test was made with enough I_2 excess to sustain *in situ* chemical vapor transportation but not too much to keep it below 15atm.

Table 4: Vapor transportation reactant quantities test 2

Compound	CeO_2	Al	I_2
Mass (mg)	173	67	995

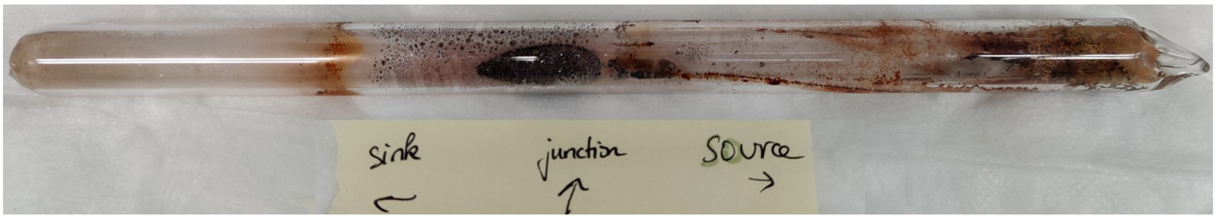

Figure 12: Vapor Transporation Test 2. Left is sink, middle is the junction between the two furnaces, right is the source

The red coloration of the products shows the clear excess of Iodine. The sink (cold) side concentrates a fine yellow powder deposit – probably crystals, the middle zone has purple crystals, probably condensed excess iodine, and the source (hot) side shows a red bulk phase which is probably aluminum oxide and iodine mixed together.

Dysprosium(II) Iodide synthesis

Synthesis

The synthesis of DyI_2 is inspired by the large scale synthesis of Dysprosium (II) Iodide proposed by Evans *et al.* [7]. Flakes of $Dy_{(m)}$ are directly reacted with I_2 following the reaction : $Dy_{(m)} + I_{2(s)} \rightarrow DyI_{2(s)}$

Since the setup by Evans *et al.* required a quartz crucible and an open furnace which weren't available in the lab, an attempt to simplify the setup was made. The reactants were transferred in quartz tubes inside an argon-filled glove bag to avoid oxidation of the metal. The tubes were subsequently sealed on a schlenk line under vacuum, then heated directly with a CH_4+O_2 flame torch. A bright glow and bubbles were noticeable. Iodine had the tendency to move to the colder end of the tube, and recrystalize. The formation of a white-pink deposit was also noticeable. When heated by the flame, the deposit would be displaced and reform on a colder surface of the tube.

Figure 13: Quartz tube with Dy(m) and I2(s) heated directly by flame torch. The heat triggers the reaction which produces the bright glow at the right side of the tube.

Two types of batches were tested based on the following quantities :

Table 5: Reactant quantities for the synthesis of DyI2

	$Dy_{(m)}$ mg	mmol	$I_{2(s)}$ mg	mmol
Small batch, ampoule volume = 3.85cm^{-3}	19.5	0.12	30.45	0.12
Big batch, ampoule volume = 7.693cm^{-3}	78	0.48	121.8	0.48

DyI_2 is known to look like a purple black solid, while DyI_3 is known to look like a green solid.

Figure 14: Quartz tube after flame treatment. Metallic bulk with purple shades on the left, white-pink layer deposit on the right.

P-XRD was ran on both the metallic bulk and on the white-pink layer deposit. See **Results**

Reduction of Cerium(III) Iodide with Dysprosium(III) Iodide

Despite the uncertain nature of the compounds, an ampoule of the cerium experiments and another one of the dysprosium experiments were both transferred into a glovebox cut open, and scraped. The products were ground and then put together in a new wide borosilicate ampoule, which was then sealed on a schlenk line under vacuum. About 50mg of the metallic bulk of the Dysprosium tube was used. The ground powder had a purple shade which hints that DyI_2 was present. About 80mg of the lime-green powder of the Cerium tube was used. The ampoule was then put in a tube furnace at 450°C overnight. No reaction was observed.

Uranium(III) Iodide synthesis

Synthesis

The synthesis of U(III) Iodide was based on the article of *Kraus et al.[6]*, first without the chemical vapor transport reaction step. The first attempts were made at low partial pressure of I_2. Similar to the Cerium(III) Iodide synthesis, the reactants were introduced in the borosilicate tubes, which were then sealed under vacuum on a schlenk line. The tubes were then put in a tube furnace and were put through a Ramp A cycle. (see Cerium Iodide Synthesis)

Table 6: Reactant quantities for synthesis of UI3 depending on the type of batch

	$UO_{2(s)}$ mg	mmol	$Al_{(m)}$ mg	mmol	$I_{2(s)}$ mg	mmol
Small batch, ampoule volume = $10cm^{-3}$	22.11	0.082	5.34	0.198	43.6	0.172
Large batch, ampoule volume = $20cm^{-3}$	221.1	0.82	53.4	1.98	436.5	1.72

Figure 15: Small batch ampoule, Left : showing green oily deposits, Right : shiny metallic unknown crystals

Figure 16: Big batch ampoule showing black dendrites on both ends, dark green deposits, and black bulk at the center

The ampoule was scored and opened in a glovebox. P-XRD analysis was done on the black dendrites and on the metallic bulk. It was assumed that the small green deposits were probably U_3O_8. See **Results**.

In situ chemical vapor transport reaction

An attempt to recrystallize and separate the products *via in situ* chemical vapor transport reactions was made. The dedicated fumehood couldn’t accomodate two furnaces so the setup had to be adapted.

A tube which had already reacted following ramp A was placed back in the furnace so that one end was right at the middle of the cavity, and the other end was sticking out of about 2cm of the furnace. To avoid too much of a sharpt temperature difference, a little bit of glass wool was wrapped around the segment at the junction inside/outside. The furnace was programmed to remain at 350°C (source) while the room temperature remained at approximatively 20°C (sink). The tube was left under these conditions for 48h before being allowed to reach room temperature without a specific ramp. P-XRD was ran on the grey-purple deposit present on the sink side. See **Results**.

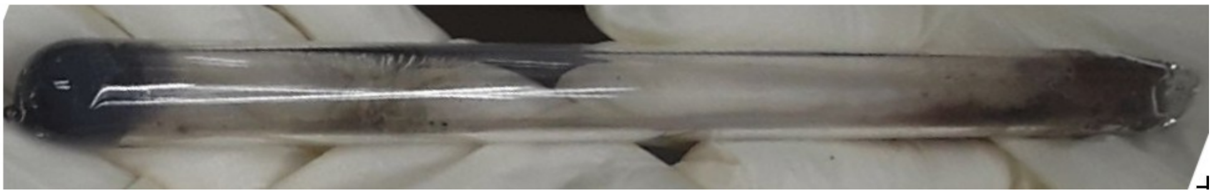

Figure 17: Ampoule after chemical vapor transport reaction for 48h with Source : 350°C - Sink : 20°C. The left end (sink) has a grey-purple deposit. A black shiny bulk is on the right end (source)

Another vapor transportation reaction was conducted over 5 days and resulted in a more defined seperation, with the appearance of what seems to be AlI_3 white crystals at the sink side. Al_2O_3 would not be mobile at such low temperatures.

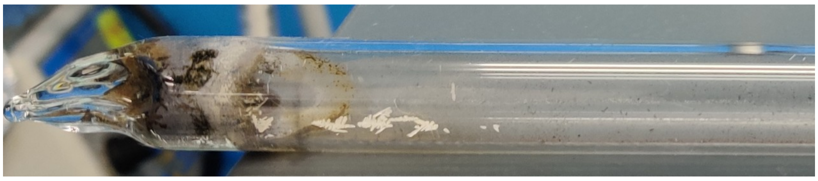

Figure 18: Ampoule after chemical vapor transport reaction for 5 days with Source : 350°C - Sink : 20°C. Presence of white dendrite crystals

Arc Melting of Cerium(III) Iodide

A first attempt to sublime iodine using the arc melter by quickly reaching temperatures over 1000°C was made. The method was based on the protocol described by Idell *et al*[3] at Lawrence Livermore National Lab. CeI_3 melting point is 766°C. Although there is no data available on the boiling point of CeI_3, as the boiling point of I_2 being 184.3 °C, it is reasonable to assume that reduction of CeI_3 can occur. It is also reasonable to assume that $Ce_{(m)}$ won't vaporize, as the boiling point of Cerium is 3443°C. (All melting and boiling point given are at atmospheric pressure).

Pure CeI_3 granules purchased from Sigma Aldrich as well as a fragment of Fe and a fragment of Zr are placed in the cavities of a costum-drilled copper mount. Both Fe and Zr fragments are used as getters. The amperage is set to 20A. Once the copper mount is in place, the arc melting chamber is purged 3 times with $Ar_{(g)}$ and then maintend under a pressure of 50 kPa $Ar_{(g)}$. The Zr fragment is melted first to captate the residual O_2. The Fe fragment is then melted to captate the expected released $I_{2(g)}$. Finally, the arc is circled around the $CeI_{3(s)}$ granules without hitting them directly and the Fe bead is regularly re-arced to stay in liquid state, until the granules fuse together to create a grey mass with yellow remnants. The arc is sustained for typically one minute.

After allowing the chamber and hearth to cool down, the chamber is opened, and the Fe and Zr beads are discarded. We observe a white deposit on all the surface of the chamber which is probably an oxide. The molten granules of CeI_3 are quickly put in vial and brought into a glovebox since CeI_3 is a hydrogyroscopic compound, and $Ce_{(m)}$ can quickly get oxidized.

A first experiment was made with 20mg of starting $CeI_{3(s)}$ material. An attempt to study the sample by SEM was made. In the glovebox, the biggest granule was rinsed with a 0.1M nitric acid solution, placed on carbon tape, and sealed under argon atmosphere. However, the sample oxidized during the transfer to the SEM chamber and no result could be extrapolated.

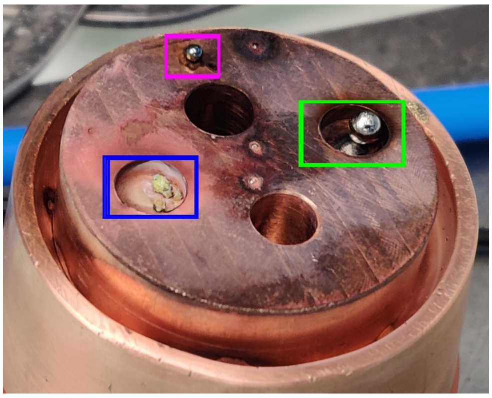

Figure 19 : Copper hearth after arc melting of CeI_3 *granules. Fused granules (blue), iron bead (green), zirconium bead (pink).*

Figure 20: Chamber post-arc. The glass is covered with a red deposit as well as with small black crystals, which seem to confirm the sublimation and deposition of I_2 *.*

A second attempt was made with 200mg of starting $CeI_{3(s)}$. This time the fused grey granules were dropped in liquid epoxy. Once cured, the excess epoxy was sawed down and the surface was polished, exposing the surface of the granules. Unfortunately, the granules seemed to oxidise right away, even when mineral oil was used as a lubricant on the sanding paper.

This can be explained by the fact that cerium is one of the most reactive rare-earth element. As described by Hammond[2] : “It is malleable, and oxidizes very readily at room temperature, especially in moist air”.

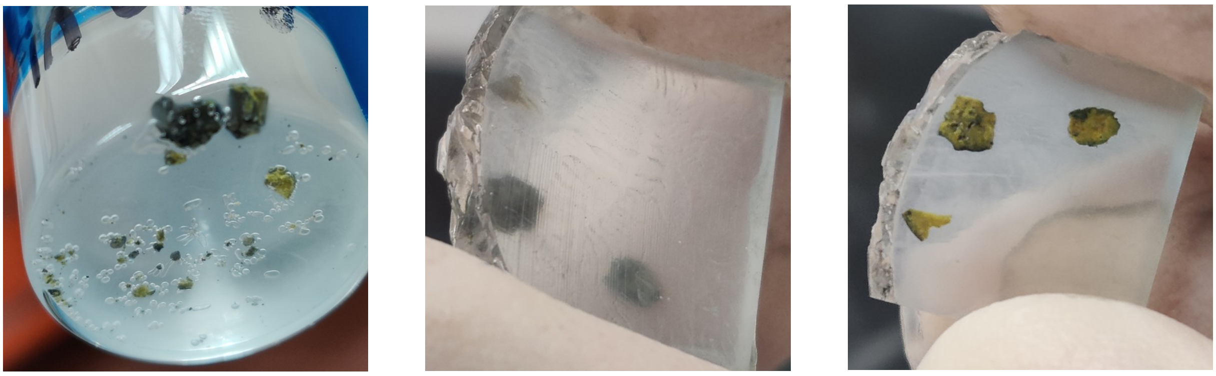

Figure 21 : Left - *Molten granules dropped in epoxy.* Center - *Unexposed grey surface of the molten granules suggesting metalic nature.* Right - *Exposed yellow polished surface of the molten granules suggesting oxidation.*

A third attempt to arc melt CeI_3 was made, this time about 30mg of granules were ground to a very fine powder prior the arc melting. It resulted in a grey powder as well as very little beads. All the material was dropped in mineral oil and brought into a glovebox. Unfortunately the tiny beads spalled once taken out from the mineral oil, so no further analysis could be done.

Arc Melting of Uranium(IV) Oxide

The arc melting of UO_2 was inspired by the work of Anderson *et al[8]* who were studying the decomposition of UO_2 at its melting point.

UO_2 powder synthesized by Phillip Hammer was pressed into pellets and put in the arc melting chamber following the same procedure as the arc melting of CeI_3. However only a Zr getter was used. Two different masses and amperage were tried. The first test was made on approximately 300mg of UO_2, with an amperage of 25A, and sustaining the arc for more than 1min. The second test was performed on about 100mg of UO_2, this time at 20A and the arc was also sustained for more than one minute.

Figure 22: UO_2 pellet post-arc with shiny spots and puffed surface

We noticed a change in the structure of the pellets. They appeared to have small shiny spots under the light, and they exhibited a porous structure. The post-arc pellets were dropped in epoxy, and after curing and sawing of the excess epoxy, the surface was smoothed with sand paper. However it appeared that the pellets were very brittle and that the surface was too easily sandable. This indicated that the pellets probably weren't $U_{(m)}$ but probably a form of UO_{2-x}.

Arc Melting of Uranium(III) Iodide

The method was based on the protocol described by Idell *et al*[3] at Lawrence Livermore National Lab. Considering that the melting point of UI_3 is 766°C, that the melting point of $U_{(m)}$ is 1132.2°C and that its boiling point is 4131°C, it was reasonable to assume that I_2 would sublime and leave the $U_{(m)}$ remaining in the copper hearth.

60mg of impure UI_3 synthesized previously were used. The fragment of UI_3 as well as the Zr and Fe getters were placed in the chamber, which was purged 3 times like in other arc melting experiments. The UI_3 fragment was arc melted at 20A for more than a minute, then allowed to cool down. Once back to room temperature, the chamber was cleaned (glass, crucible, electrode) and the UI_3 fragment was placed again in the chamber with new getters. The fragment was arc melted a second time, this time at 22A for more than a minute. The resulting fragment was analysed through SEM. See **Results**.

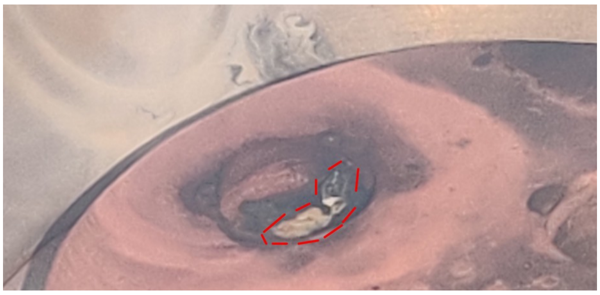

Figure 23: Post-arc UI_3 fragment. The red dotted circle outlines a shiny grey element which might be metal.

Results

Cerium Iodide(III) synthesis

P-XRD was run on the red powder deposit. The analysis indicated that the ramp B seemed to produce CeO_2 with extra I_2 trapped in it. The diffractogram didn't show another compound, and the air-tight dome ended up being colored purple, most probably because of the gradual release of I_2.

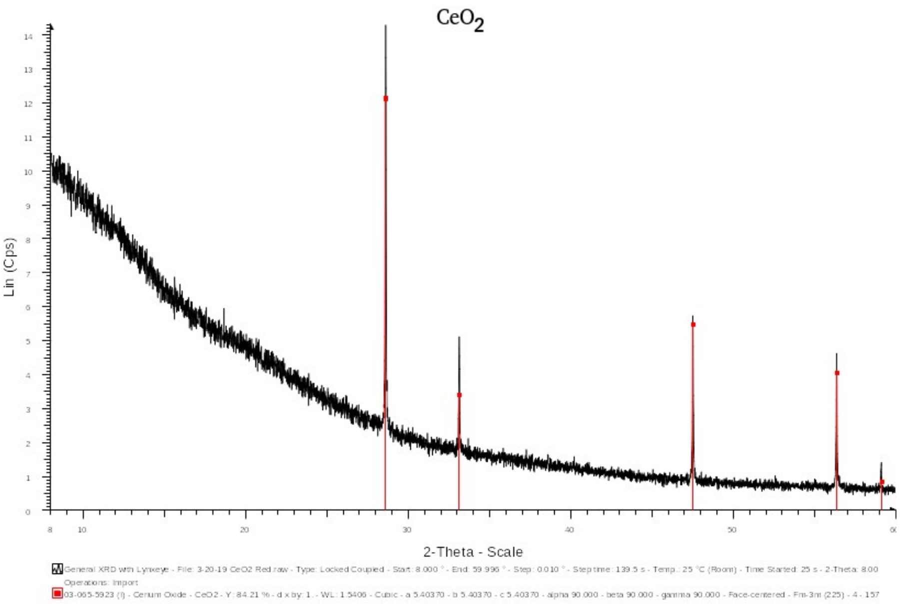

Figure 24: Diffractogram of red powder deposit resulting from CeI_3 synthesis experiment with Ramp B, showing univocal match with CeO2. Red peaks belong to the CeO_2 diffractogram from the database.

As for the yellow-lime crystals obtained from experiments with Ramp A, they look exactly similar to the pure CeI_3 granules purchased from Sigma Aldrich. Coupled with the 3 sub-experiments which confirmed the reaction pathway, it is safe to assume that the yellow-lime crystals are CeI_3 crystals with residual Al_2O_3 contamination (white deposits).

Dysprosium Iodide synthesis

P-XRD was run on the two different product phases : the metallic bulk, and the white-pink deposit. The two phases are clearly different compounds as shows the non-matching superimposition of the two diffractograms.

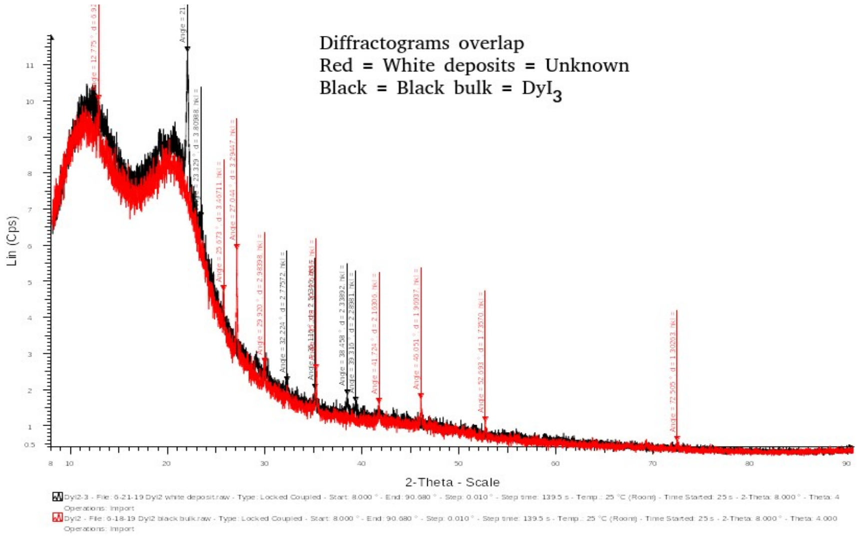

Figure 25: Superimposition of the two diffractograms from the Dysprosium Iodide synthesis. Red corresponds to the white-pink deposit and Black to the metallic bulk.

The metallic bulk seems to be mainly DyI_3 as it matches the DyI_3 diffractogram available in the database. Unfortunately the reaction didn't seem to have produced DyI_2 despite the fact that the ground bulk resulted in a purple powder and not green one, which should indicate the presence of DyI_2 and not DyI_3.

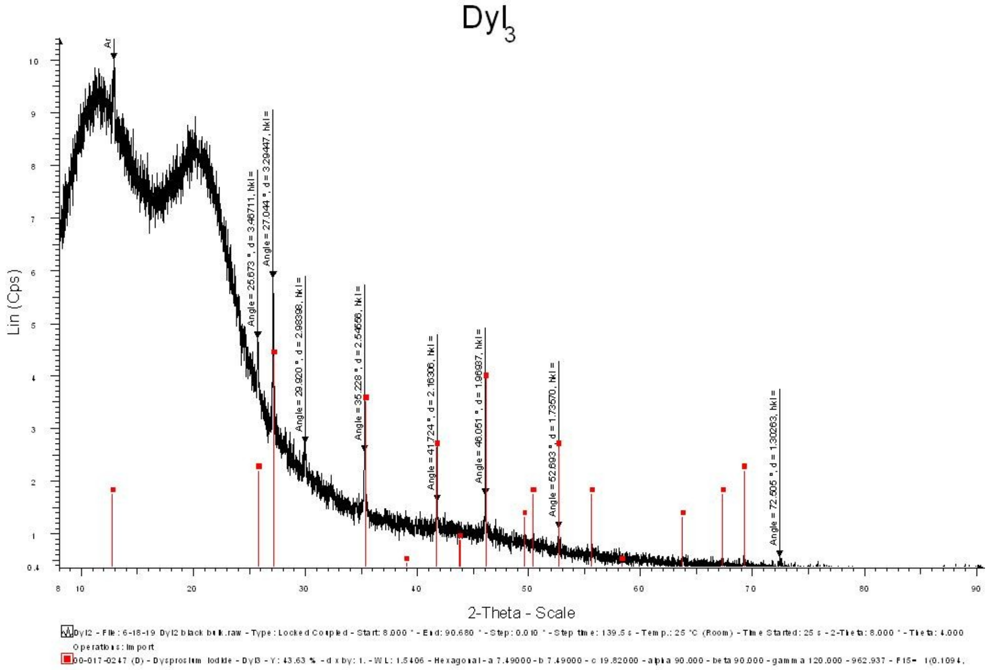

Figure 26: Diffractogram of metallic bulk phase from Dysprosium Iodide synthesis. The red peaks belong to the DyI_3 diffractogram from the database.

The second phase made of white pink deposits which was found in each iteration of the synthesises didn't find a match in the database. The scope of potential compounds was widened by taking into account other possible elements which could have contaminated the reaction. Even when considering boron, silicium, oxygene and hydrogren, there was still no match in the database.

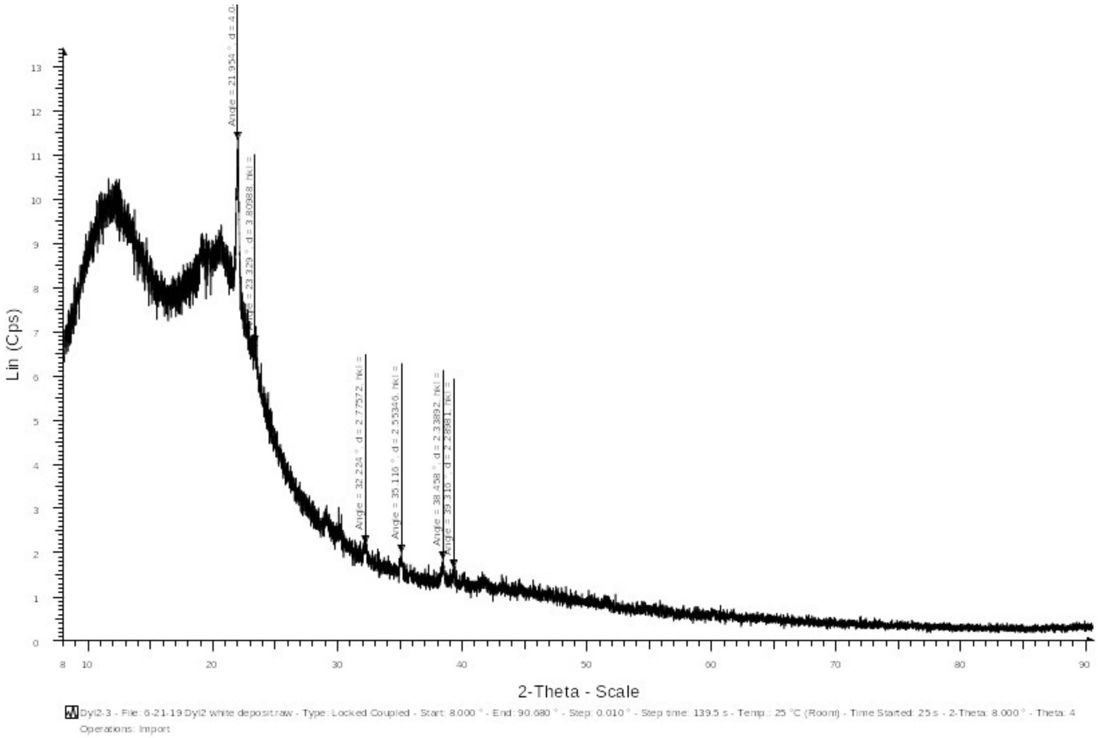

Figure 27: Diffractogram of the white deposit from Dysprosium Iodide synthesis. No match was found in the database.

Uranium Iodide synthesis

Synthesis

<u>P-XRD :</u>

The two main phases were studied with P-XRD. Despite appearing like crystal dendrites, the black dendrites didn't show any crystalinity. Their nature couldn't be determined.

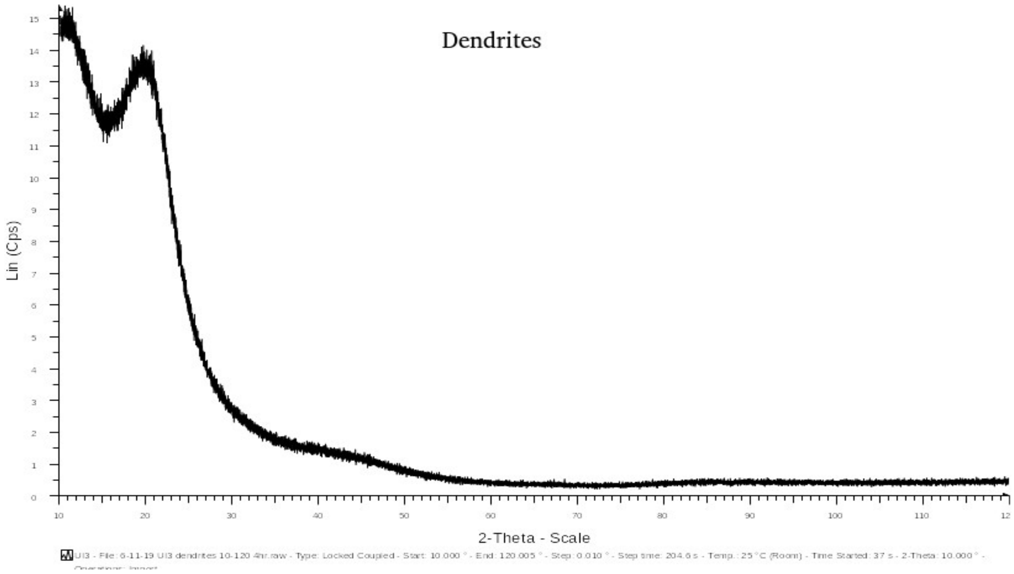

Figure 28: Diffractogram of dendrites from UI_3 synthesis experiment.

As for the metallic bulk phase, it showed a match with the UI_3 diffractogram in the database. However, the UI_3 signal is weak and accompanied with several other peaks, which suggests it's not pure and mixed with other compounds. It is safe to assume that the contaminating compounds are Al_2O_3, I_2, and maybe AlI_3 and $Al_{(m)}$ remnants.

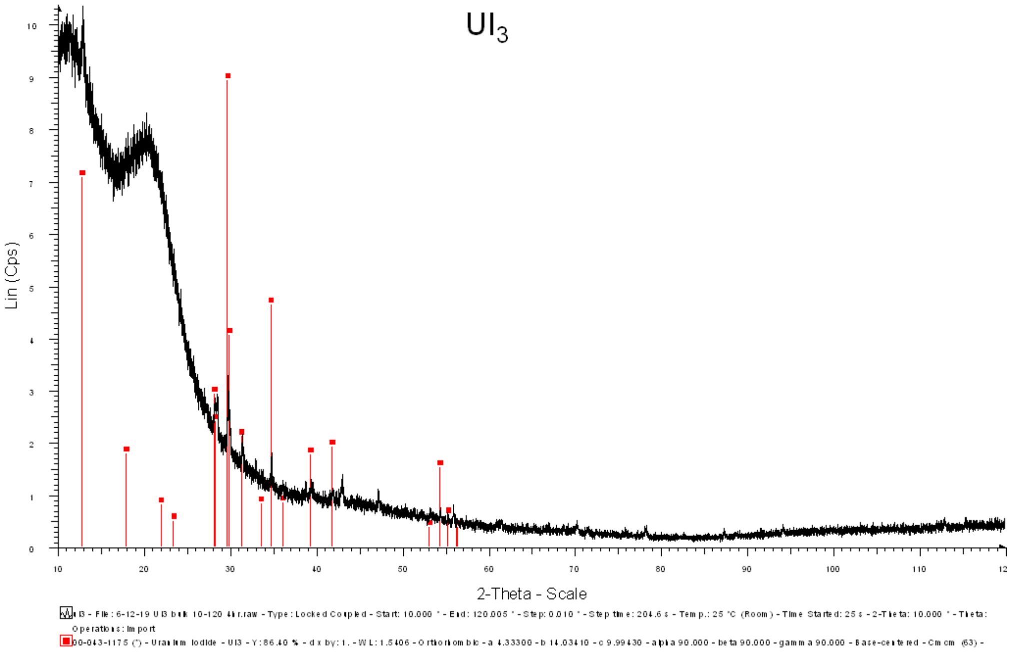

Figure 29: Diffractogram of the metallic bulk phase of the UI_3 synthesis experiment. Red peaks belong to the UI_3 spectrum available in the database.

SEM:

A small amount of the metallic bulk was ground and analysed with an SEM. Elemental analysis was performed on several spots.

We notice a ratio 1:3 of U:I which seems to confirm the presence of UI_3. The high percentage of oxygen can be explained by the oxidation of the sample during the transfer to the SEM chamber, the presence of Al_2O_3, and unreacted UO_2.

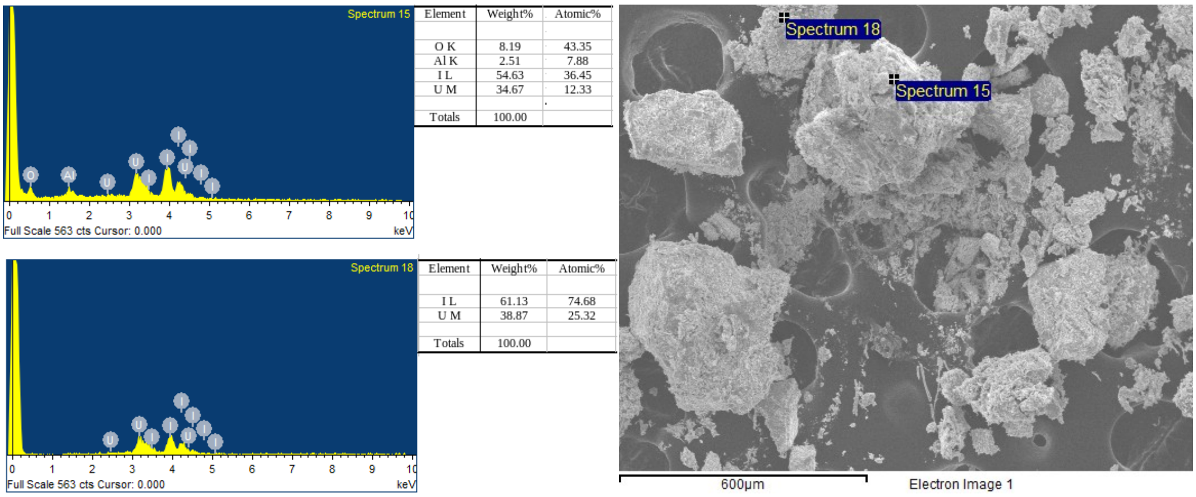

Element	Weight%	Atomic%
O K	8.19	43.35
Al K	2.51	7.88
I L	54.63	36.45
U M	34.67	12.33
Totals	100.00	

Element	Weight%	Atomic%
I L	61.13	74.68
U M	38.87	25.32
Totals	100.00	

Figure 30: Elemental analysis of the ground bulk phase showed that it is roughly U:I 1:3, with some Al and O present. Voltage = 15kV, magnification = 75

In situ chemical vapor transport reaction

The grey-purple deposit found on the sink side after the *in situ* chemical vapor transport reaction was analyzed by P-XRD. It appeared to be AlI_3 which was not found on the previous diffractograms of the UI_3 synthesis.

It seems to indicate that the vapor transport reaction leads to the isolation of this intermediate compound by transporting it from the bulk to the cold end. This means that the setup as it is acts as a preliminary purification and seperation method for UI_3.

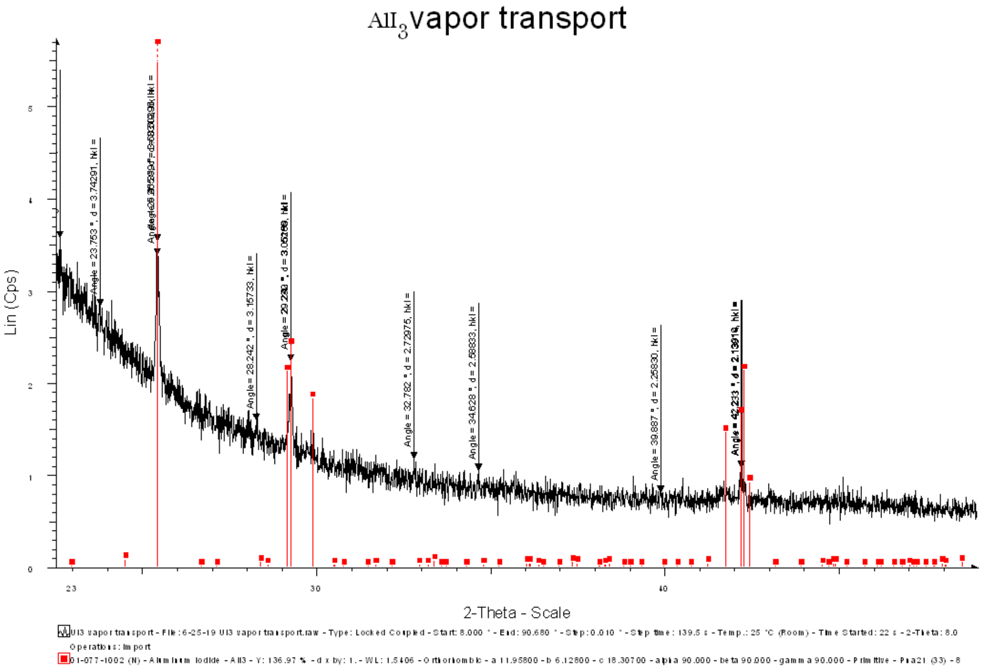

Figure 31: Diffractogram of AlI_3 isolated through chemical vapor reaction.

Reduction of Cerium(III) Iodide with Dysprosium(III) Iodide

No chemical reaction was observed.

Cerium(III) Iodide Arc Melting

No analytical data could be extracted. The sample would oxidize before reaching the SEM chamber or P-XRD stage. Other analytical methods such as chemical titration need to be explored in order to determine the oxidation state of the Ce, as well as the presence of other elements.

Uranium(III) Iodide Arc Melting

The metallic fragment obtained after the arc melting of UI_3 was brought to SEM for elemental analysis. The element mapping revealed that most of the Iodine had disappeared and had left clear patches of Uranium with remaining Aluminum and Oxygen contamination. The Aluminum and Oxygen are found together and overlap on the same areas which further suggests the presence of Al_2O_3.

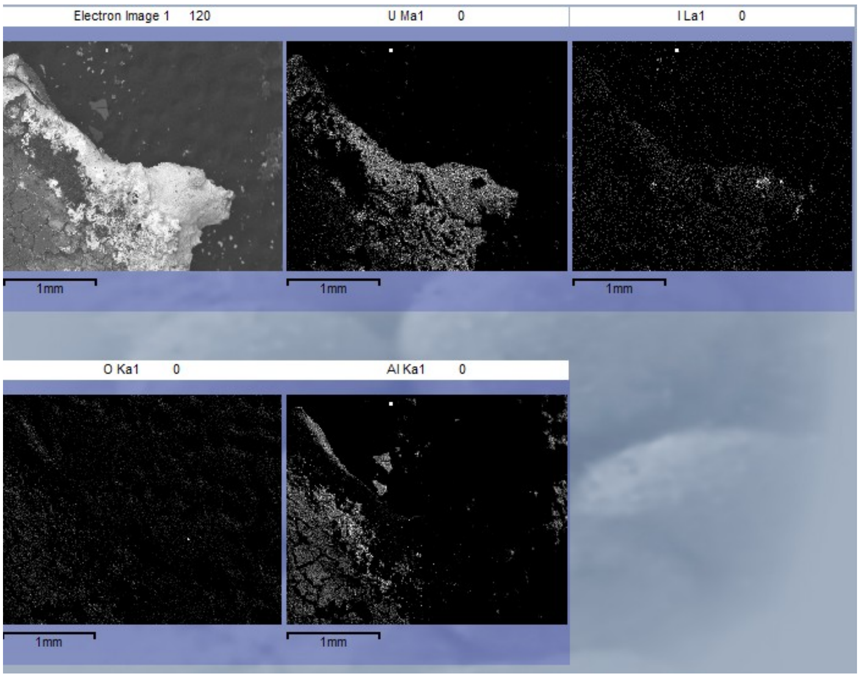

Figure 32: SEM element maps of post-arc UI3 fragment. Top left is the electron image of the sample, the other maps show the elements U, I, O, and Al.

Five different locations of the sample were mapped, and the resulting average atomic percentages are presented on the figure below. It shows that Iodine is almost non-existant (less than 1%) which means that arc melting is a successful technique to reduce UI_3 to $U_{(m)}$ by sublimation of I_2. It also shows that the Al:O ratio is about 2:3 which is consistent with the presence of Al_2O_3.

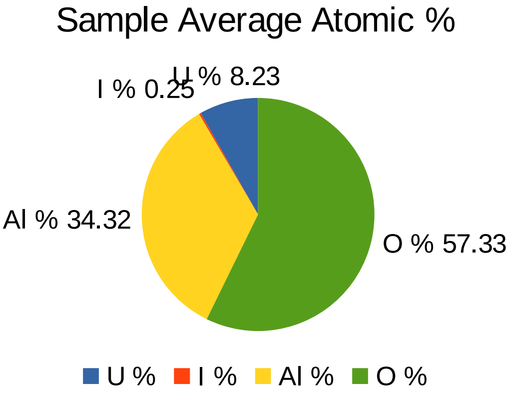

Conclusions

The synthesises of CeI_3 and UI_3 were successful. They will require further efforts in order to isolate and purify the compounds of interests from the other products. This might be solved by the purchase of a tube furnace whith internal temperature gradient and longer *in situ* vapor transportation reactions. The synthesis of DyI_2 was unsuccessful and will require to modify the setup. The DyI_3 and CeI_3 showed no reaction at 450°C, which suggests that DyI_3 doesn't exhibit reduction properties under these conditions, contrary to DyI_2.

The arc melting of CeI_3 and UI_3 were succesful. The metallic nature of the post-arc Cerium fragment needs additional effort to be confirmed. As for the arc melting of UI_3, the recovery yield of $U_{(m)}$ needs to be quantified by reproducing the experiment with different amounts of starting material.

The arc melting of UO_2 didn't lead to $U_{(m)}$ recovery but clear changes were observed on the samples, namely a puffed surface and small shiny spots, which might indicate that the compound turned to a UO_{2-x} composition. Working at a higher amperage with lower quantities might improve the reduction. Designing a funnel-like copper hearth might improve the recovery of $U_{(m)}$ which could sink and drop at the bottom as it is denser than the starting material.

Finally, the arc melting reduction approach should be extended to other Cerium and Uranium halides, such as $CeBr_3$, $CeCl_3$, UCl_3, UCl_4 or UBr_4.

References

Bibliography

1: Moody K. J., Hutcheon I. D., Grant P. M., *Nuclear Forensics Analysis*, CRC Press Book, 2005;

2: Hammond C. R., The Elements in *Handbook of Chemistry and Physics*, CRC Press Book , 2000

3: Idell Y. S., Holliday K. S., Stillwell R. L., Jeffries J. R., Reduction of uranium triiodide to metal by thermal decomposition, *Journal of Radioanalytical and Nuclear Chemistry*, **2019**, 320, 793–800

4: Atkins P.W., Shrivee, D. F., The f-elements in S*hriver & Atkins' inorganic chemistry*, 5th Ed, Oxford University Press, 2010

5: Shannon, R. D., Revised effective ionic radii and systematic studies of interatomic distances in halides and chalcogenides, *Acta Crystallographica Section A: Foundations and Advances,* **1976**, 32, 751–767

6: Kraus F., Rudel S. S., Deubner L. H., Scheibe B., Conrad M., Facile Syntheses of pure pure uranium halides: UCl4 , UBr4 and UI4, *Zeitschrift für anorganische und allgemeine Chemie,* **2018**, 644, 323–329

7: Evans W. J., Allen N. T., Workman P. S., Meyer J. C., Large Scale Synthesis of Dysprosium and Neodymium Diiodides, *Inorganic Chemistry*, **2003**, 42 (9)

8: Anderson J. S., Sawyer J. O., Worner H. W., Willis G. M., Bannister M. J., Decomposition of Uranium Dioxide at its Melting Point, *Nature,* **1960**, 185, 915–916